

Atomic Scale Oxidation of a Complex System: $O_2/\alpha\text{-SiC}(0001)\text{-}(3 \times 3)$

F. Amy,¹ H. Enriquez,¹ P. Soukiassian,¹ P.-F. Storino,² Y. J. Chabal,² A. J. Mayne,³ G. Dujardin,³
Y. K. Hwu,⁴ and C. Brylinski⁵

¹*Commissariat à l'Energie Atomique, DSM-DRECAM-SPCSI-SIMA, Bâtiment 462, Saclay,
91191 Gif sur Yvette Cedex, France*

and Département de Physique, Université de Paris-Sud, 91405 Orsay Cedex, France

²*Bell Laboratories, Lucent Technologies, 600 Mountain Avenue, Murray Hill, New Jersey 07974*

³*Laboratoire de Photophysique Moléculaire, Université de Paris-Sud, Bâtiment 210, 91405 Orsay Cedex, France*

⁴*Academia Sinica, Nankang, Taipei, Taiwan*

⁵*THALES, Laboratoire Central de Recherches, Domaine de Corbeville, B.P. 10, 91401 Orsay Cedex, France*

(Received 10 October 2000)

The atomic scale oxidation of the $\alpha\text{-SiC}(0001)\text{-}(3 \times 3)$ surface is investigated by atom-resolved scanning tunneling microscopy, core level synchrotron radiation based photoemission spectroscopy, and infrared absorption spectroscopy. The results reveal that the initial oxidation takes place through the relaxation of lower layers, away from the surface dangling bond, in sharp contrast to silicon oxidation.

DOI: 10.1103/PhysRevLett.86.4342

PACS numbers: 81.65.Mq, 68.37.Ef

Semiconductor surface passivation, while of central importance to microelectronic and optoelectronic device technologies, is poorly understood at a fundamental level. In particular, the ultrathin silicon oxides required for the latest very-large and ultralarge scale integration CMOS technologies are finally approaching the fundamental limits. At this level, it is essential to understand the degree of homogeneity achievable and the nature of stress induced upon oxidation. While a large amount of work has been done on silicon oxidation due to the remarkable interfacial properties of silicon/SiO₂ [1–3], the situation is generally very different for other semiconductors such as III-V and IV-IV compounds, which do not have high quality native oxides and/or the high interfacial quality.

In this view, silicon carbide (SiC) is of special interest. SiC is a wide band gap IV-IV compound semiconductor, existing in hexagonal (α), cubic (β), and rhombohedral phases [4]. SiC has advanced characteristics making it especially suitable for high temperature, high power, high voltage, and high frequency electronic devices and sensors [4], and there is an urgent need to understand the initial oxidation at the atomic scale. The challenge lies in the complexities of both the surfaces and the oxidation processes themselves. So far, there is only one study on initial oxygen interaction on the $\alpha\text{-SiC}$ surface using conventional Auger, electron energy loss, and diffraction techniques primarily devoted to the effect of B on surface reactivity [5]. For the present study, we therefore combine three complementary advanced techniques to unravel the initial oxidation of a particularly complex system, the 3×3 reconstructed $\alpha\text{-SiC}(0001)$ surface. Its structure includes a twisted Si adlayer above a bulk SiC substrate with Si tetramers (Si trimer + Si adatom) on top [6], as shown in Fig. 1.

In this Letter, we show that, in contrast to silicon surfaces, the $\alpha\text{-SiC}(0001)\text{-}(3 \times 3)$ readily oxidizes at very low oxygen exposures away from the top layer atoms (i.e.,

dangling bonds). The oxygen migrates to a deep silicon layer closer to the bulk carbon plane. Furthermore, oxidation is shown to relieve the surface strain, again in sharp contrast to silicon oxidation, suggesting that, ultimately, the formation of a more homogeneous oxide is possible.

Scanning tunneling microscopy (STM) was performed in an ultrahigh vacuum Omnicron instrument, core level photoemission spectroscopy (CLPS) at the Synchrotron Radiation Research Center (Hsinchu, Taiwan) and infrared absorption spectroscopy (IRAS) at Bell Laboratories. The use of these three complementary techniques is crucial. While STM is a powerful tool for atomic scale real space investigations, oxidation studies are often a challenge as the observation of reacted sites cannot always be linked to a specific oxygen configuration [7,8]. To the extent that core level shifts can be directly linked to the oxidation state [9,10], CLPS complements STM by providing precious chemical information. However, charge transfer arising from relaxation or bonding rearrangement in strained SiC surfaces may also cause core levels to shift. IRAS is therefore also required to obtain evidence for oxygen insertion [3,11]. Strong lattice and free carrier absorption in doped SiC dictate a 45° incidence reflection geometry for IRAS, providing submonolayer sensitivity to modes perpendicular to the surface in the 650–950 cm⁻¹ range only [12]. Both 6H and 4H $\alpha\text{-SiC}(0001)\text{-}(3 \times 3)$ surfaces, which are known to have the same 3×3 surface structure, were prepared by repeated Si deposition and thermal annealing sequences [4,6,9,13].

The effects of low oxygen exposures on the $\alpha\text{-SiC}(0001)\text{-}(3 \times 3)$ surface are first investigated with STM. Figure 2 displays 300 Å × 300 Å STM topographs (filled electronic states) for clean 2(a) and O₂ exposed 2(b) and 2(c) $\alpha\text{-SiC}(0001)\text{-}(3 \times 3)$ surfaces. In agreement with previous studies [6,14], the clean surface shows large spots in hexagonal array, with one single spot per unit cell representing the adatom + trimer structure. The most

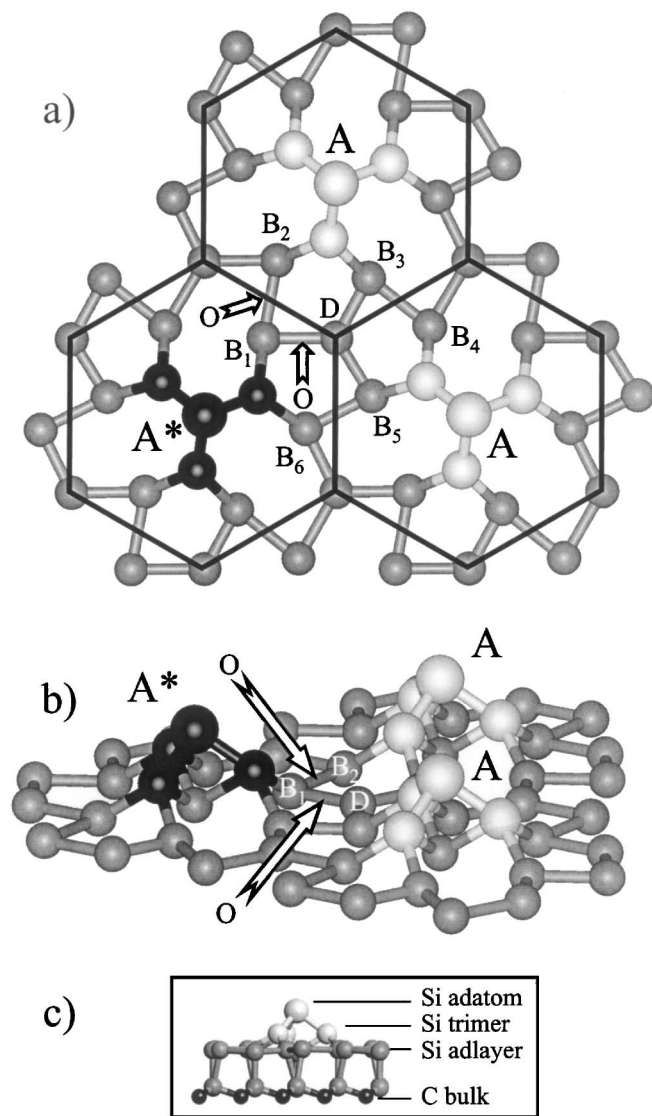


FIG. 1. Schematic of (a) top and (b) side views of the α -SiC(0001)-(3 \times 3) reconstruction (after Ref. [6]) showing adatom, trimer, and Si adlayer and layer planes and the proposed D-O-B₁ and B₁-O-B₂ initial bonding site for oxygen atoms. A and A* represent the bright and dark sites observed in STM, respectively. For clarity, the three first Si atomic planes have been represented only on the side view (b), but all planes above the C plane are represented in the inset (c).

common defects on the clean surface appear as bright and dark spots, corresponding to excess and reduced electron density, respectively. Upon 0.25 L (1 L = 1 Langmuir = 10^{-6} torr \cdot s) oxygen exposure [Fig. 2(b)], new bright and/or dark spots appear away from the original bright or dark spots, in contrast to the cubic β -SiC(100)-(3 \times 2) surface where an initial bright defect is the preferred adsorption site for oxygen [8]. A comprehensive statistical defect analysis of several series of STM topographs, with a set representative ones shown in both Figs. 2(b) and 2(c), reveals that the bright sites seem to be created preferentially in pairs (side by side) rather

than in an isolated manner, each pair being associated with a nearby dark site (in 94% of the cases). This leads to the creation of patches of several reacted sites forming a hexagonal arrangement looking similar to “flowers” arranged side by side, with the bright spots forming the petals [Fig. 2(c)].

Using well-established peak decomposition, Si 2*p* and C 1*s* core level shifts during low oxidation regime are key to identifying oxygen atom location with the unit cell. For the clean, α -SiC(0001)-(3 \times 3) reconstructed surface [Fig. 3(a)], the Si 2*p* exhibits a bulk (100.18 eV) and two surface shifted components SS1 and SS2 [13]. SS1 (98.75 eV) is associated with the Si adatom and SS2 (99.41 eV) to the Si trimer + Si adlayer [13] of the recently accepted 3 \times 3 model [6].

Upon very low (0.25 L) O₂ exposure [Fig. 3(b)], the Si 2*p* core level shape is significantly affected with a new chemically shifted component located at 100.43 eV binding energy corresponding to Si⁺ oxidation state. This

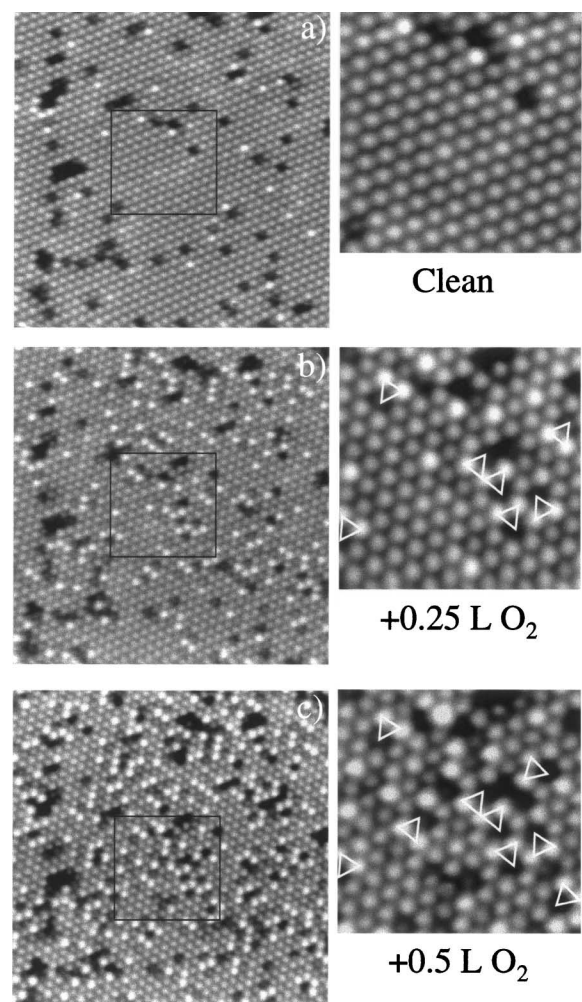


FIG. 2. 300 \AA \times 300 \AA (left) and detailed 100 \AA \times 100 \AA (right) STM filled state topographs for the α -SiC(0001)-(3 \times 3) (a) clean surface and oxygen exposed at (b) 0.25 L and (c) 0.5 L. Triangles indicate pairs of bright sites (A) associated with a dark site (A*).

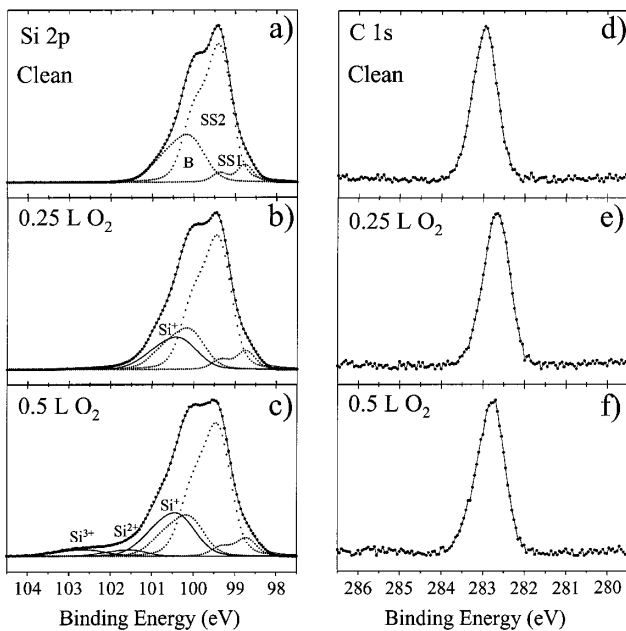


FIG. 3. Si $2p$ core level for the α -SiC(0001)-(3 \times 3) (a) clean surface and oxygen exposed at (b) 0.25 L and (c) 0.5 L in the surface sensitive mode ($h\nu = 150$ eV and emission angle and $\theta_e = 30^\circ$). (d), (e), (f): C $1s$ core level for the same surfaces as in (a), (b), and (c) ($h\nu = 330$ eV and emission angle and $\theta_e = 60^\circ$).

indicates that we are not in a chemisorption regime, but already in an oxidation one at exposures significantly lower than for other semiconductors [10]. At 0.5 L, two weaker components with larger shifts are detected at 101.54 eV (Si^{2+}) and 102.66 eV (Si^{3+}) [Fig. 3(c)] and indicate formation of small amounts of higher Si oxidation states, even at low exposure.

The Si $2p$ core level results clearly show that there is oxidation at low exposures and that the components associated with the adatom (SS1) and trimer (SS2), i.e., the two topmost surface layers, are unaffected by this initial oxidation. This implies that the oxygen atoms interact with Si atoms located below the first two surface layers to form an oxide structure in the third layer. This view is consistent with the rather low number of surface reacted sites that could be observed in the above STM topographs (Fig. 2), suggesting that the dark and bright spots observed in STM result from electronic effects rather than from direct oxygen interaction with surface or subsurface atoms.

A 0.3 eV shift to lower binding energy of the C $1s$ core level [Figs. 3(d)–3(f)] during the same exposure sequence, and a 10% broadening after 0.25 L O_2 exposure [Fig. 3(e)], indicates that the first C atoms, located in the fifth atomic plane far away from the topmost Si surface atoms are slightly affected by oxygen incorporation. This further supports a picture of O atoms migrating well below the surface, leaving the trimer/adatom structure unaffected as clearly observed in the sharp 3 \times 3 low energy electron diffraction pattern after 0.25 L O_2 exposure or above.

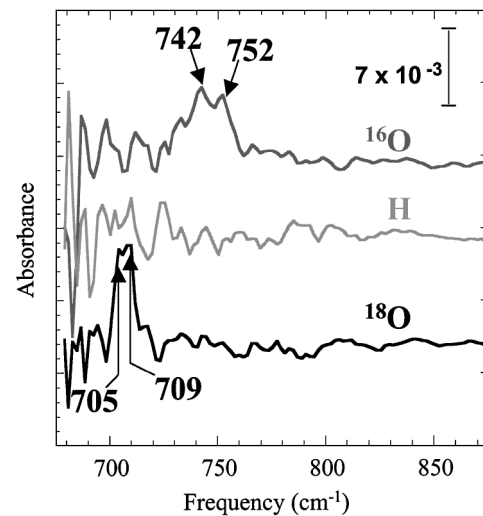


FIG. 4. Infrared reflection absorption spectra of α -SiC(0001)-(3 \times 3) after (top) exposure to 0.25 L of ^{16}O (oxygen 16), (center) to 2L of atomic H (using 150 L of H_2), and (bottom) 0.15 L of ^{18}O (oxygen 18).

The reactivity of the surface to low oxygen exposures is confirmed by infrared absorption spectroscopy. In the range of 0.2 to 1 L of $^{16}\text{O}_2$, two absorption features are observed at 742 and 752 cm^{-1} , and at 705 and 709 cm^{-1} upon 1 L $^{18}\text{O}_2$ exposure, as shown in Fig. 4. Their frequencies, strengths, and characteristic isotopic shifts are consistent with symmetric stretch vibrations of two distinct Si-O-Si structures within a surface unit cell [11]. These features are altered at higher exposures (>1 L), consistent with further incorporation and therefore vibrational interaction of additional oxygen within the unit cell. Interestingly, an unusual Fano feature has also been identified at 904 cm^{-1} on the clean α -SiC(0001)-(3 \times 3) surface (not shown) and been assigned to a coupling of the highest frequency adatom/trimer normal mode with the adatom dangling-bond associated electronic band transition [15]. This feature disappears upon H exposure and is substantially affected by high oxygen exposures, but is unaffected during the initial exposure regime (<1 L), precisely in the range where the 742 and 752 cm^{-1} modes are observed. These observations taken together suggest that initial oxidation occurs by oxygen insertion into bridge sites away from the adatom/trimer structure, in excellent agreement with the above Si $2p$ and C $1s$ core level shifted component behavior.

The results obtained with STM, CLPS, and IRAS can be correlated while considering the specific structure of the 3 \times 3 surface reconstruction (Fig. 1). Since the reaction between oxygen and Si atoms occurs below the surface, the bright/dark sites that are created result from charge redistribution associated with the reaction underneath. We generally observed that two bright sites are created together with a dark one, these three sites being nearest neighbor spots in the STM topographs (Fig. 2). This indicates that each of these three spots, representing adatom + trimer

atoms (A), is affected by the oxygen reaction with an atom underneath. One should notice here that all B atoms, the nearest atoms bonded to the trimer atoms, do not have strictly identical bonding, with different bond angles [6] due to the adlayer rotation (Fig. 1). The group "A" atoms give the STM topographs spots which could be bright A or dark A^* . Having these three A groups affected by oxygen must result from an asymmetric charge redistribution from oxygen-silicon atom bonding. In this context, atom D is of special interest since it is at the "center of gravity" of the three A groups. In addition, atom D which belongs to the Si adlayer, is far from the ideal sp^3 configuration with a vertical backbond to the underlying Si plane while the three other bonds (to B_i atoms) are equivalent and horizontal [6]. These features suggest that the D atom or its neighboring B atoms are likely to be initially affected by an oxygen atom. IRAS makes it possible to discriminate among these various possibilities. The modes at 742 and 752 cm^{-1} indicate two bridge bonding configurations, without the involvement of the trimer atoms since the Fano feature is unaltered and the Si-O-Si symmetric stretch modes are mostly polarized perpendicular to the surface. The existence of two distinct oxygen vibration modes clearly suggests D-O-B and B-O-B bonding configurations, as represented in Fig. 1 as, e.g., D-O- B_1 and B_1 -O- B_2 . In the oxidation process, D could approach a more ideal sp^3 bonding configuration with the formation of a D-O-B bond, lowering the surface energy through strain relief. This would, in turn, result in additional charge transfer from D toward the Si adlayer and also to the carbon plane as indicated by the 0.3 eV shift of the C 1s core level [Fig. 3(e)]. However, such an effect is more difficult to detect at Si 2p due to composition with chemical shift related to O atoms bonding.

The above picture of D-O- B_1 and B_1 -O- B_2 bond formation would account for the observation of a dark A^* site in STM pictures (Figs. 1 and 2). Indeed, the two oxygen (D-O- B_1 and B_1 -O- B_2) atoms bonded to B_1 will induce charge depletion resulting in a A^* to B_1 charge transfer leading to a dark spot in the STM image. The formation of the two bright A sites is most likely linked to the strain relief induced by oxidation, leading to charge redistribution in the two other A structures of the unit cell.

In conclusion, the atomic scale initial oxidation of α -SiC(0001)-(3 \times 3) has been unraveled, pointing to dramatic differences with silicon oxidation. Using three complementary techniques, room temperature molecular oxygen was shown to dissociate readily (<1 L), with subsequent incorporation in to the lower silicon layer far away from the only dangling bond associated with the top adatom/trimer layers. Furthermore, in contrast to Si, this initial oxidation is likely to relax the highly strained SiC surface, suggesting that a more uniform silicon oxide layer can be produced on SiC than on Si surfaces. Finally, this

work suggests that even the interfaces of more complex technological materials of the future can now be studied when combining a number of state-of-the-art techniques.

This work was supported in part by the Institute Français de Taipei (IFT), by the National Science Council (NSC, Taipei), and by the DGA (Paris, France). It is based upon research conducted in part at the Synchrotron Radiation Research Center (SRRC), Hsinchu, Taiwan. The authors are especially grateful to the SRRC staff for expert and outstanding assistance and to Dr. Tseng for the use of his experimental system.

-
- [1] S. M. Sze, *Modern Semiconductor Devices Physics* (Wiley, New York, 1998).
 - [2] *Fundamental Aspects of Ultrathin Dielectrics on Si-based Devices*, edited by E. Garfunkel, E. Gusev, and A. Vul', NATO Science Series, Vol. 3 (Kluwer, Dordrecht, 1998).
 - [3] M. K. Weldon, K. T. Queeney, Y. J. Chabal, B. B. Stefanov, and K. Raghvachari, *J. Vac. Sci. Technol. B* **17**, 1795 (1999).
 - [4] *Silicon Carbide, A Review of Fundamental Questions and Applications to Current Device Technology*, edited by W. J. Choyke, H. M. Matsunami, and G. Pensl (Akademie-Verlag, Berlin, 1998), Vols. I and II.
 - [5] V. M. Bermudez, *Appl. Surf. Sci.* **84**, 45 (1995).
 - [6] K. Reuter, J. Bernhardt, H. Wedler, J. Schardt, U. Starke, and K. Heinz, *Phys. Rev. Lett.* **79**, 4818 (1997); U. Starke, J. Schardt, J. Bernhardt, M. Franke, K. Reuter, H. Wedler, K. Heinz, J. Furthmuller, P. Käckell, and F. Bechstedt, *Phys. Rev. Lett.* **80**, 758 (1998).
 - [7] J. P. Pelz and R. H. Kock, *Phys. Rev. B* **42**, 3761 (1990); R. Martel, Ph. Avouris, and I. W. Lyo, *Science* **272**, 385 (1996); G. Dujardin, A. Mayne, G. Comtet, L. Hellner, M. Jamet, E. Le Goff, and P. Millet, *Phys. Rev. Lett.* **76**, 3782 (1996); I. S. Hwang, R. L. Lo, and T. T. Tsong, *ibid.* **78**, 4797 (1997).
 - [8] A. Mayne, F. Semond, G. Dujardin, and P. Soukiassian, *Phys. Rev. B* **57**, R15 108 (1998).
 - [9] F. Amy, P. Soukiassian, Y. K. Hwu, and C. Brylinski, *Appl. Phys. Lett.* **75**, 3360 (1990).
 - [10] Z. H. Lu, M. J. Graham, S. P. Tay, D. T. Jaing, and K. H. Tan, *J. Vac. Sci. Technol. B* **13**, 1626 (1995), and references therein.
 - [11] B. B. Stefanov, A. B. Gurevich, M. K. Weldon, K. Raghavachari, and Y. Chabal, *Phys. Rev. Lett.* **81**, 3908 (1998).
 - [12] The external reflection geometry dictated by the sample precludes the observation of the corresponding asymmetric modes because of a dramatic decrease in surface sensitivity in the 950 to 1200 cm^{-1} region.
 - [13] F. Amy, P. Soukiassian, Y. K. Hwu, and C. Brylinski, *Surf. Sci. Lett.* **464**, L691 (2000).
 - [14] M. A. Kulakov, G. Henn, and B. Bullemer, *Surf. Sci.* **346**, 49 (1996).
 - [15] P.-F. Storino and Y. Chabal, recent IRAS results (to be published).